Lab on a Chip

PAPER

View Article Online
View Journal | View Issue

Cite this: *Lab Chip*, 2014, **14**, 3101

Wireless EWOD/DEP chips powered and controlled through LC circuits and frequency modulation

Sung-Yueh Wu and Wensyang Hsu*

Received 7th April 2014,
Accepted 4th June 2014

DOI: 10.1039/c4lc00421c

www.rsc.org/loc

This paper presents novel wireless EWOD/DEP chips that are wirelessly powered and controlled through LC circuits with one-to-many transmitter–receiver coupling. Each receiving LC circuit connected to the EWOD/DEP electrode is designed to have a different resonant frequency. When the input frequency is close to one of the resonant frequencies of receiving LC circuits, the induced voltage on the corresponding EWOD/DEP electrode will increase due to the resonance. Therefore, electrodes can be selectively and sequentially activated to provide sufficient EWOD or DEP force to manipulate the droplet or liquid by modulating the input frequency. Unlike previously reported wireless EWOD or DEP devices powered through one-to-one transmitter–receiver coupling, the transmitting inductor in the one-to-many transmitter–receiver coupling design proposed here is much larger than the total sizes of receiving inductors. Therefore, receiving inductors can be easily covered and coupled by the transmitting inductor. Here, droplet transport, splitting, and merging are successfully demonstrated using 5 receiving LC circuits at different input frequencies (1210–1920 Hz). Liquid pumping with multiple electrodes by wireless DEP is also demonstrated using 5 receiving LC circuits at higher input frequencies (51.2–76.1 kHz). Furthermore, liquid pumping with a continuous meandered electrode by wireless DEP is demonstrated through the resonant frequency shifting effect. It shows that the liquid pumping distance on a continuous electrode also can be tuned by proper frequency modulation.

1. Introduction

Liquid manipulation on a micro scale has been carried out through continuous flows in physical microchannels, which may suffer from complicated systems that consist of channels, valves and a pumping source.[1,2] On the other hand, electrokinetic forces, electrowetting on dielectric (EWOD) and dielectrophoresis (DEP), have been attractive alternative approaches to handle microfluidics, since their *in situ* driving forces and open structures obviate the pumping and leakage problems, which are commonly encountered in continuous-flow systems with closed physical channels. EWOD provides a versatile and flexible tool to manipulate droplets. Many microfluidic functions by EWOD have been realized, such as creating, transporting, splitting, and merging droplets.[3–5] DEP, a technique to manipulate polarizable particles in liquids by non-uniform electric fields,[6–9] is also capable of manipulating liquid in continuous forms.[10]

Recently, wireless EWOD and DEP devices have been reported.[11–17] Without a battery or other power supply electrically connected to the devices, the placement of EWOD/DEP devices can be more flexible. Mita *et al.* presented the first wireless EWOD device to move the bubble on a pond skater through a LC circuit.[11,12] By using the one-to-one transmitter–receiver design, droplet transportation by wireless EWOD was also realized through an amplitude-modulation method.[13–16] In addition to wireless EWOD, bead concentration by wireless DEP was achieved through integration of a printable RF circuit and a bead-based DEP device.[17] However, liquid pumping or manipulation through wireless DEP has not been reported yet.

Here, a one-to-many transmitter–receiver coupling design is developed to achieve droplet manipulation using the wireless EWOD device through LC circuits and frequency modulation. Furthermore, liquid pumping through wireless DEP is also realized for the first time. Unlike previously reported wireless EWOD or DEP devices powered through one-to-one transmitter–receiver coupling, the external transmitting inductor proposed here is much larger than the total sizes of receiving inductors in the one-to-many transmitter–receiver coupling design. Therefore, receiving inductors connected to wireless EWOD/DEP chips can be easily covered and coupled by the transmitting inductor.

2. Concept design

To realize wireless EWOD/DEP chips powered and controlled through one-to-many transmitter–receiver coupling, a novel design that integrates LC circuits and an EWOD/DEP device

Department of Mechanical Engineering, National Chiao Tung University, 1001 Ta Hsueh Road, Hsinchu 30010, Taiwan. E-mail: whsu@mail.nctu.edu.tw

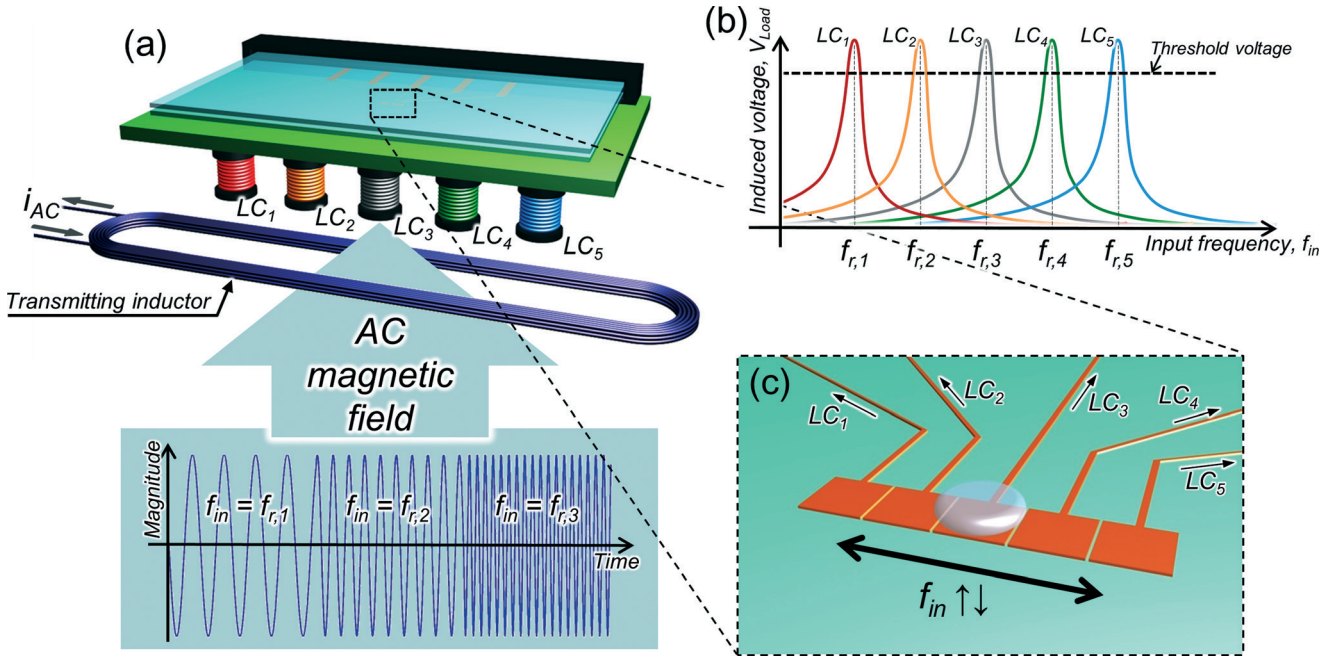

Fig. 1 Schematic diagram of the proposed wireless EWOD/DEP chip: (a) one-to-five transmitter–receiver coupling, (b) induced different voltages through frequency modulation, (c) microfluidic manipulation on electrodes with different resonant frequencies.

is proposed, as shown in Fig. 1(a). By applying an alternating current (AC) signal with input frequency f_{in} to a transmitting inductor, oscillating magnetic flux is generated in nearby space. Due to near-field inductive coupling between the transmitting inductor and receiving LC inductors, electric energy can be wirelessly induced in receiving LC circuits. Receiving LC circuits with different resonant frequencies are electrically connected to the corresponding electrodes on EWOD/DEP devices. Signals with voltage V_{Load} and frequency f_{in} are wirelessly induced on receiving LC circuits and corresponding electrodes. If the input frequency f_{in} is close to one of the resonant frequencies f_r of receiving LC circuits, the induced voltage V_{Load} of the LC circuit increases due to the resonance. If the induced voltage V_{Load} is larger than the threshold voltage of the EWOD/DEP device, sufficient EWOD/DEP forces can be generated to manipulate droplet or liquid. Since each receiving LC circuit has different resonant frequencies and frequency responses, induced voltages in receiving LC circuits can be different from each other. Therefore, the specific LC circuit can be selectively charged to exceed the threshold voltage of the EWOD/DEP device, as shown in Fig. 1(b) and to manipulate droplet or liquid by modulating the input frequency f_{in}, as shown in Fig. 1(c).

3. Design and fabrication

The equivalent circuit diagram of the proposed wireless EWOD/DEP chip is shown in Fig. 2(a). With a function generator producing an AC signal with input frequency f_{in} to control the power amplifier, the oscillating current with the same frequency f_{in} can be sent into the transmitting inductor. Due to near-field coupling between one transmitting inductor and several receiving inductors, that is, one-to-many transmitter–receiver coupling, forward electromotive forces are induced wirelessly in every receiving LC circuit based on Faraday's law. Each receiving LC circuit is connected to the top plate and a corresponding bottom electrode of the EWOD/DEP device.

EWOD, a technique used to change the wettability of a dielectric solid surface by applying a voltage across the dielectric layer, is commonly utilized to manipulate micro droplets. A common design of the EWOD device is also shown in Fig. 2(a), which is a closed arrangement composed of a patterned bottom plate with dielectric and hydrophobic layers, as well as a top plate with the unpatterned electrode layer and hydrophobic layer. By applying sufficient voltage across the dielectric layer V_D, the droplet can be moved due to the electrodynamic forces.[18]

DEP, which has been widely employed to manipulate polarizable particles, is also capable to provide surface forces to continuously draw dielectric liquid of higher permittivity along a strong DC electric field into the region of lower permittivity, such as air.[19–25] A high-frequency AC electric field was also found to be able to drive aqueous liquids between parallel electrode plates coated with dielectric layers against gravity by enough voltage drop across the liquid V_L, which means that EWOD and DEP can be realized in the same device that contains dielectric-coated electrodes,[21–23,26] as shown in Fig. 2(a).

To make the EWOD/DEP device, both the top and bottom plates are fabricated from indium-tin-oxide (ITO) glass. To pattern the bottom plate for electrodes, lithography and etching

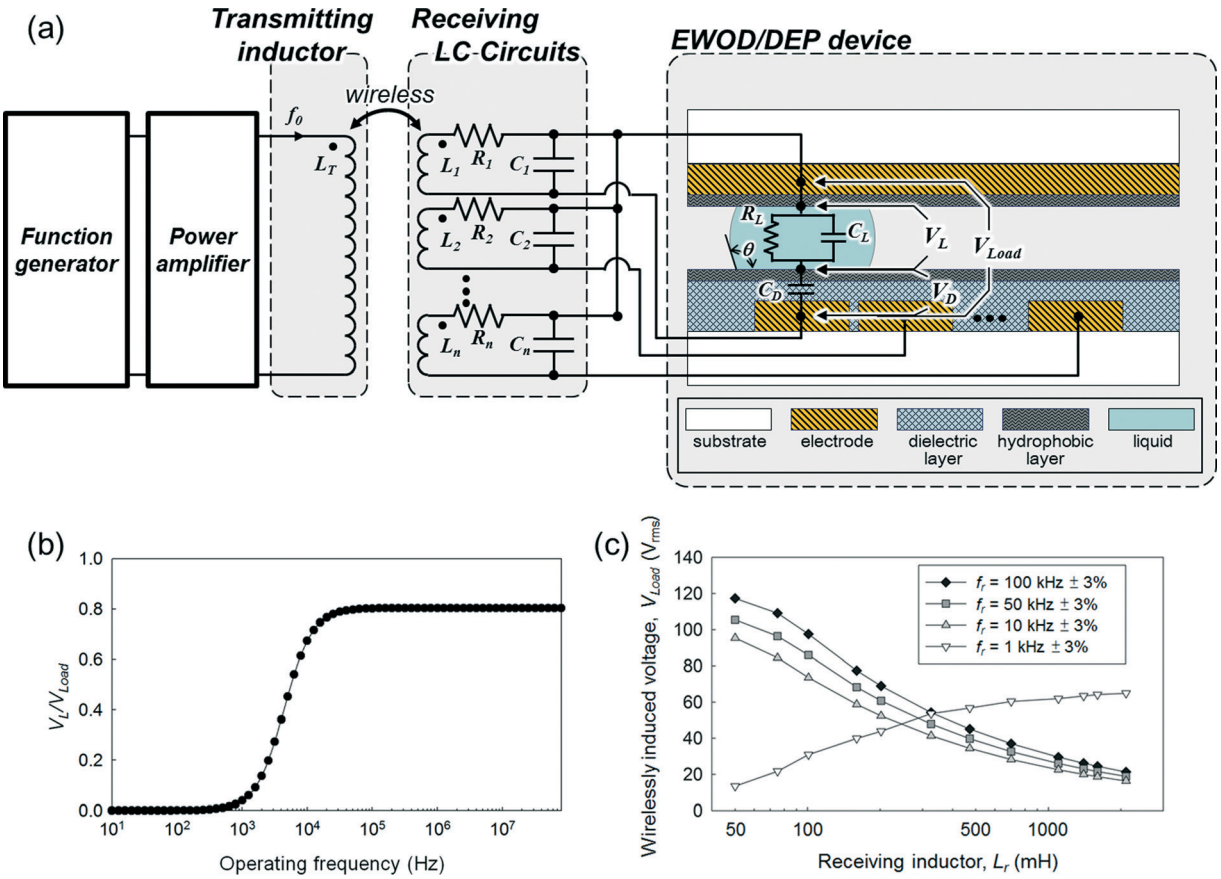

Fig. 2 Detailed design of the proposed wireless EWOD/DEP chips: (a) equivalent circuit diagram and cross-sectional view of the EWOD/DEP device, (b) the frequency-dependant voltage curve of the EWOD/DEP device, (c) measured wirelessly induced voltages with different inductors under different resonant frequencies.

processes are carried out using photo resist FH-6400 (Fujifilm Olin) and *aqua regia*. After taping part of the electrodes, the 1.6 μm dielectric layer SU-8 2002 (MicroChem) is spun, exposed, and baked (160 °C for 10 minutes). To further deposit the hydrophobic layer, 5% Teflon (DuPont Teflon AF 1600 diluted by 3M FC-770) is spun. After baking at 160 °C for 20 minutes, the fabrication of hydrophobic layer is achieved with a thickness of 70 nm. After removing the tape, the fabrication of the bottom plate is completed. The top plate is fabricated using a similar process but without the patterning of the electrode and the deposition of the dielectric layer. The gap between the top and bottom plates is controlled by a spacer with a thickness of 150 μm (MISUMI SFGSML 0.15). The width and gap of the EWOD square electrode are 1000 μm and 20 μm, respectively. The width of the electrode pattern for DEP is 200 μm. Then the fabricated EWOD/DEP devices are wired and tested to obtain threshold voltages. It is found that threshold voltages of EWOD and DEP devices are 55 V_{rms} and 80 V_{rms}, respectively. The maximum droplet transporting speed of the wired EWOD device is found to be 6120 μm s^{-1} with switching frequency 6 Hz.

To design appropriate receiving LC circuits for EWOD/DEP, following approaches are performed: (1) obtain the appropriate operating frequency range for EWOD/DEP; (2) measure the threshold voltages of fabricated EWOD/DEP devices and test different kinds of receiving inductors under EWOD/DEP frequencies. For different liquids, the above approaches can be used to find those key parameters.

3.1 Operating frequency

To provide EWOD forces, most of the induced voltage V_{Load} needs to drop across the dielectric layer. To generate the DEP force, a drop in V_{Load} needs to happen across the liquid. To further clarify the voltage–drop relationship, an analytical model, as listed in eqn (1),[27] is used, which is affected by the operating frequency f, dielectric layer capacitance C_D, liquid capacitance C_L, and liquid resistance R_L. For the fabricated EWOD/DEP device with deionized water as the liquid ($\sigma_l = 1 \times 10^{-4}$ S m^{-1}, $\varepsilon_l = 80$), the frequency-dependent voltage–drop curve is simulated, as shown in Fig. 2(b). The cut-off frequency, f_c, based on eqn (2),[27] is found to be around 4.4 kHz. When an AC signal with an operating frequency below the cut-off frequency is applied, the voltage drop across the liquid (V_L) is almost zero. It means the entire applied voltage drops across the dielectric layer, which is helpful to cause EWOD. On the other hand, to realize the DEP phenomenon, the resonant frequencies of receiving LC circuits should be

higher than the cut-off frequency to have a larger V_L/V_{Load} ratio to ensure a sufficient voltage drop across the liquid.

$$\frac{V_L}{V_{Load}} = \mathrm{Re}\left(\frac{j2\pi f C_D R_L}{1 + j2\pi f (C_D + C_L) R_L}\right) \quad (1)$$

$$f_C = \frac{1}{2\pi R_L (C_L + C_D)} \quad (2)$$

3.2 Receiving LC circuit

To induce voltages larger than threshold voltages in resonance, especially in the low frequency range for EWOD, the inductance of the receiving LC circuit needs to be large enough for a good quality factor. Therefore, inductors with a ferromagnetic core, which can increase the inductance by a factor of several thousand through high magnetic permeability of the magnetic core, are selected as receiving inductors for EWOD/DEP devices. Using the function generator Agilent 33210A to control the signal waveform, the power amplifier can output signal with the same frequency and larger current. In the in-house power amplifier, the signal is amplified using an operational amplifier (Texas Instruments OPA454) first and then sent to transistors (STMicroelectronics 2N3055 and MJ2955) to control the current output.[28] Providing ±15 V_{DC} to the operational amplifier and transistors, 0.037–1.21 A_{AC} with frequency 100–1 kHz can be sent to a transmitting inductor (inductance 440 μH and resistance 5.7 Ω) with length 16 cm and width 2 cm, which is made by winding the enameled insulated wire (diameter 0.51 mm) for 15 turns. Corresponding waveforms, impedances, and currents are measured using Agilent oscilloscope DSO 1004A, impedance analyzer 4294A, and multimeter 34401A, respectively.

At the wireless distance of 1.0 cm between the transmitter and receiving inductors, induced voltages of different LC circuits are measured, as shown in Fig. 2(c). At low resonant frequency, 1 kHz, larger inductances are found to induce higher voltage. For higher resonant frequency, 10–100 kHz, smaller inductances are found to induce higher voltage. Therefore, for the proposed wireless EWOD device, where low operating frequency (<4.4 kHz) is needed, the receiving inductor larger than 300 mH is selected to produce an induced voltage larger than the EWOD threshold voltage, 55 V_{rms}. For wireless DEP, where high operating frequency (>4.4 kHz) is needed, the receiving inductor smaller than 90 mH is selected to produce an induced voltage larger than the DEP threshold voltage, 80 V_{rms}. With inductances 2043.1 mH for EWOD and 50.3 mH for DEP, the maximum allowable wireless distances between the transmitting and receiving inductors for wireless EWOD and DEP are found to be 1.5 cm and 3 cm, respectively.

4. Testing and discussion

The fabricated device and testing setup are shown in Fig. 3(a). The transmitting inductor is mounted on a movable platform for easy handling. The transmitting inductor is about 16 cm in length and 2 cm in width, which is much larger than the size of whole 5 receiving inductors (length 5 cm and width 0.8 cm in total). Therefore, receiving inductors can be easily covered and coupled by the transmitting inductor. The EWOD/DEP device and receiving LC circuits are connected through printed circuit board (PCB). The operating process of the microfluidic manipulation is observed using an optical microscope. To simplify the setting procedures of receiving LC circuits, such as replacing LC circuit with different resonant frequencies, receiving LC circuits are modularized through USB mini B plugs for easy replacement, as shown in Fig. 3(b).

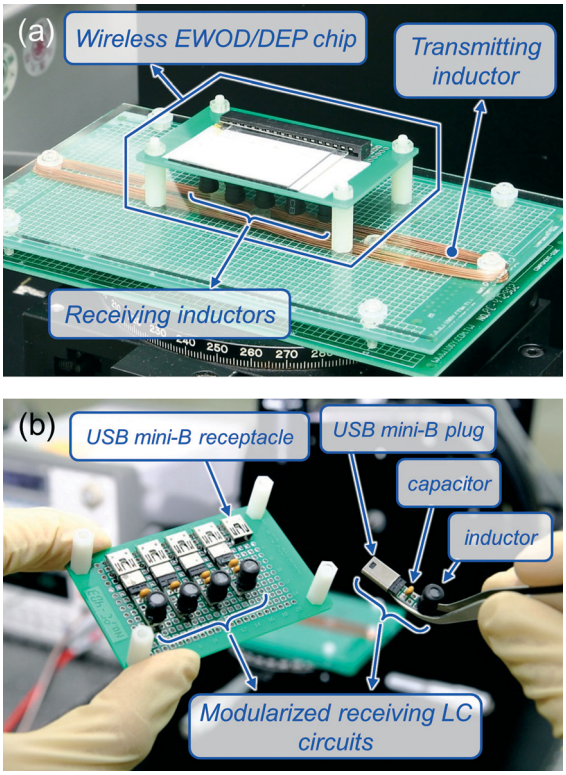

Fig. 3 Photos of wirelessly powered EWOD/DEP chips: (a) wireless EWOD/DEP chip and transmitter, (b) backside view of the wireless EWOD/DEP chip.

4.1 Wireless EWOD

To demonstrate the capability of the proposed wirelessly powered and controlled EWOD system, resonant frequencies of receiving LC circuits are designed to be below 2 kHz to have a sufficient voltage drop across the dielectric layer. Also, ferromagnetic core inductors with inductances about 2 H are selected as receiving inductors. The height and outer diameter of the receiving inductors for wireless EWOD are 13 mm and 8 mm, respectively, which are formed through winding a ferromagnetic core with an enameled wire (diameter 0.08 mm) for about 4950 turns. Here, five receiving LC circuits are designed to demonstrate droplet transport, splitting and merging functions. Different capacitors are utilized to adjust resonant

Table 1 Measured parameters of the receiving LC circuits for EWOD

LC no.	E-1	E-2	E-3	E-4	E-5
L (mH)	2043.1	2039.4	2041.5	2047.1	2045.5
C (pF)	7231.9	5802.1	4703.1	2861.7	2425.1
f_r (Hz)	1210	1370	1540	1700	1920

frequencies of LC circuits connected to different electrodes. Detailed parameters are listed in Table 1. Using a power amplifier to produce the transmitting current about 1.21 A_{AC} in our frequency range, wirelessly induced voltages at a wireless distance of 1 cm are measured and shown in Fig. 4(a). It is shown that only the receiving LC circuit at its resonant frequency can have its induced voltage larger than the EWOD threshold voltage. For example, when the input frequency f_{in} is around the resonant frequency of $LC_{E\text{-}3}$, 65.94 V_{rms} is induced in $LC_{E\text{-}3}$ and other induced voltages are all smaller than the threshold voltage of EWOD, 55 V_{rms}. As a result, the electrode connected to $LC_{E\text{-}3}$ can be selectively activated to provide EWOD forces.

The layout of the EWOD device for 1-dimensional (1D) transportation is shown in Fig. 4(b1), which has five 1000 μm × 1000 μm electrodes arranged in line with gap 20 μm. With the input frequency f_{in} switched from the lowest resonant frequency $f_{r,E\text{-}1}$ (1210 Hz) to the highest resonant frequency $f_{r,E\text{-}5}$ (1920 Hz) in sequence, the 180 nL droplet is successfully transported from the first electrode toward the fifth electrode, as shown in Fig. 4(b2–b6). With the input frequency switched from $f_{r,E\text{-}5}$ back to $f_{r,E\text{-}1}$ in sequence, the droplet is successfully moved back to the first electrode, as shown in Fig. 4(b6–b10). The proper input frequencies of EWOD are found not sensitive to the droplet capacitance, since the capacitance used here (2425.1–7231.9 pF) is much larger than the droplet capacitance, which is calculated to be about 1.2 pF. The maximum speed of the droplet movement is found to be 2040 μm s^{-1} with switching frequency 2 Hz, which is slower than the result of the wired device test, 6120 μm s^{-1}, because the induced voltage on the adjacent electrode may cause a pull-back force to slow down the droplet. To further reduce the voltage induced on the adjacent electrode, receiving LC circuits with a better resonant quality factor can be used in the future, such as using a ferromagnetic core with better magnetic permeability or adopting a wire with better conductivity. The maximum number of receiving LC circuits with different resonant frequencies is also affected by the resonant quality factor. When resonant frequencies of different receiving LC circuits are getting closer, higher voltage may be induced on the adjacent electrode to cause a larger pull-back force. A better resonant quality factor or a wider operating frequency range will be helpful to arrange more number of resonant frequencies for different receiving LC circuits without causing higher induced voltage on the adjacent electrode.

To further test the droplet splitting and merging capabilities of wireless EWOD, the layout is slightly modified, as shown in Fig. 4(c1). With the input frequency f_{in} switched from $f_{r,E\text{-}1}$ through $f_{r,E\text{-}2}$ (1370 Hz) to $f_{r,E\text{-}3}$ (1540 Hz), the 360 nL droplet successfully split to two droplets, as shown in Fig. 4 (c2–c4). With the input frequency f_{in} switched from $f_{r,E\text{-}3}$ through $f_{r,E\text{-}2}$ back to $f_{r,E\text{-}1}$, the two droplets successfully merged, as shown in Fig. 4 (c4–c6).

For 2-dimensional (2D) droplet transportation, which is also a common function in the EWOD system, the electrode layout of the EWOD device and the transporting route are designed and shown in Fig. 4(d1), which is a 3 by 5 array consisting of 15 1000 μm × 1000 μm electrodes with gap 20 μm. To transport the droplet in 2 directions, each electrode and four nearby electrodes should be connected to different LC circuits. Therefore, 5 LC circuits are also used in the 2D wireless EWOD device. Although 15 electrodes are designed as a 3 by 5 array in the 2D EWOD device, they are connected to only 5 receiving inductors arranged in line. Then one transmitting inductor is enough to cover all 5 receiving inductors, like 1D EWOD. With the input frequency switching from $f_{r,E\text{-}3}$ through $f_{r,E\text{-}4}$ (1700 Hz) to $f_{r,E\text{-}5}$, the droplet is moved to the right, as shown in Fig. 4(d2–d4). By further switching the input frequency from $f_{r,E\text{-}5}$ through $f_{r,E\text{-}2}$ to $f_{r,E\text{-}4}$, the droplet is then moved downward, as shown in Fig. 4(d4–d6). In a similar manner, the droplet can be transported along the following designed route, as shown in Fig. 4(d6–d10). Therefore, droplet transportation in 2D by wireless EWOD is successfully demonstrated by the frequency modulation method.

4.2 Wireless DEP

For wireless DEP, resonant frequencies of receiving LC circuits are designed to be higher than 50 kHz to have a sufficient voltage drop across the liquid, as shown in Fig. 2(b). Also, ferromagnetic core inductors with inductances about 50 mH are selected as receiving inductors to have larger induced voltages, as shown in Fig. 2(c). The height and outer diameter of the receiving inductors for wireless DEP are 9 mm and 5 mm, respectively, that are formed through winding a ferromagnetic core with an enameled wire (diameter 0.08 mm) for about 820 turns. The liquid pumping with multiple electrodes is tested first. Then the liquid pumping with a long continuous electrode is also investigated.

4.2.1 Liquid pumping with multiple electrodes. To demonstrate the liquid pumping capability with multiple electrodes by wireless DEP, 5 receiving LC circuits with different resonant frequencies are designed, as listed in Table 2.

With an AC current about 0.037 A_{AC} sending into the transmitting inductor, wirelessly induced voltages at a wireless distance of 1 cm are measured and shown in Fig. 5(a). It is also shown that only the receiving LC circuit at its resonant frequency can have its induced voltage larger than the DEP threshold voltage, which means that the specific electrode can be activated through frequency modulation. For example, when the input frequency f_{in} is equal to the resonant frequency $f_{r,D\text{-}2}$, 112.32 V_{rms} is induced on $LC_{D\text{-}2}$, and induced voltages on other LC circuits are all smaller than the threshold voltage of DEP, 80 V_{rms}. As a result, the electrode connected to $LC_{D\text{-}2}$ can be selectively activated to induce the DEP force.

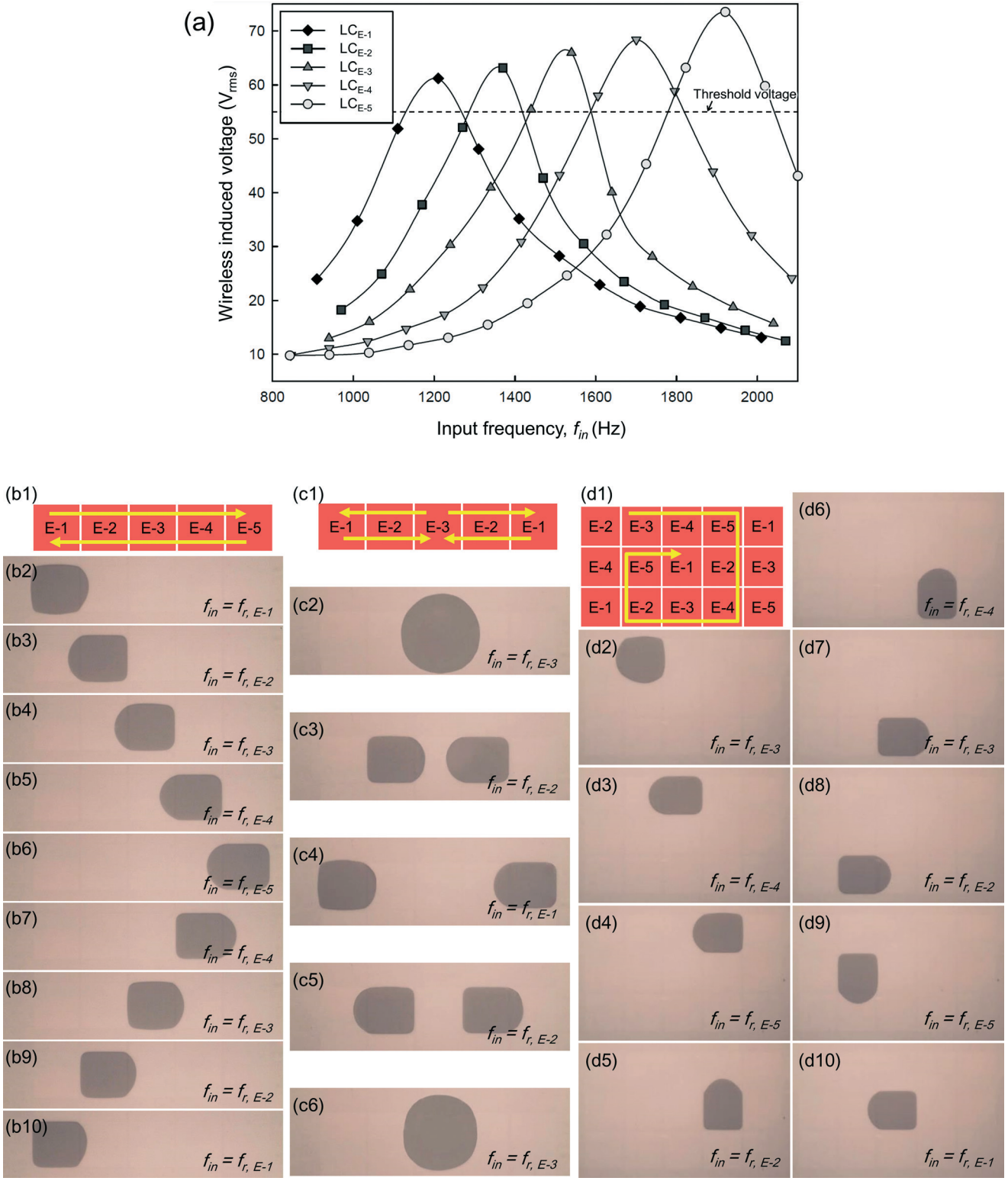

Fig. 4 Wireless EWOD: (a) wireless induced voltages on 5 receiving LC circuits of the EWOD device; (b1) the layout and designed route of 1D droplet transportation; (b2–b10) images on transporting the droplet along the designed 1D route with different input frequencies; (c1) the layout and designed route of 1D droplet splitting and merging; (c2–c6) images on splitting and merging the droplet along the designed route with different input frequencies; (d1) the layout and designed route of 2D droplet transportation; (d2–d10) images on the transport of the droplet along the designed 2D route with different input frequencies.

The electrode pattern of the DEP device is shown in Fig. 5(b), which consists of 4 rectangular electrodes with width 200 μm and a cross-shape electrode in the middle. When the input frequency is increased from $f_{r,D-1}$ (51.2 kHz)

Table 2 Measured parameters of the receiving LC circuits for DEP

LC no.	D-1	D-2	D-3	D-4	D-5
L (mH)	50.3	50.7	50.4	50.0	50.1
C (pF)	150.1	101.0	77.8	56.9	47.5
f_r (kHz)	51.2	56.7	62.5	69.2	76.1

to $f_{r,D\text{-}2}$ (56.7 kHz), the liquid channel is pumped downward to the middle, as shown in Fig. 5(c–d). With further increasing the input frequency to $f_{r,D\text{-}3}$ (62.5 kHz), the liquid channel is pumped toward the left, as shown in Fig. 5(e). If the input frequency is increased from $f_{r,D\text{-}1}$ to $f_{r,D\text{-}2}$ and switched to $f_{r,D\text{-}4}$ (69.2 kHz), the liquid is pumped downward, as shown in Fig. 5(f). Similarly, if the input frequency is increased from $f_{r,D\text{-}1}$ to $f_{r,D\text{-}2}$ and switched to $f_{r,D\text{-}5}$ (76.1 kHz), the liquid can be pumped to right, as shown in Fig. 5(g). Therefore, the liquid can be wirelessly pumped and switched through tuning the input frequency in a designed sequence. The appropriate input frequencies of DEP here are found not sensitive to the liquid capacitance, since the capacitance used here (47.5–150.1 pF) is much larger than the liquid capacitance, which is calculated to be about 0.24 pF.

4.2.2 Liquid pumping with a continuous electrode. A long continuous electrode is designed, as shown in Fig. 5(h), to

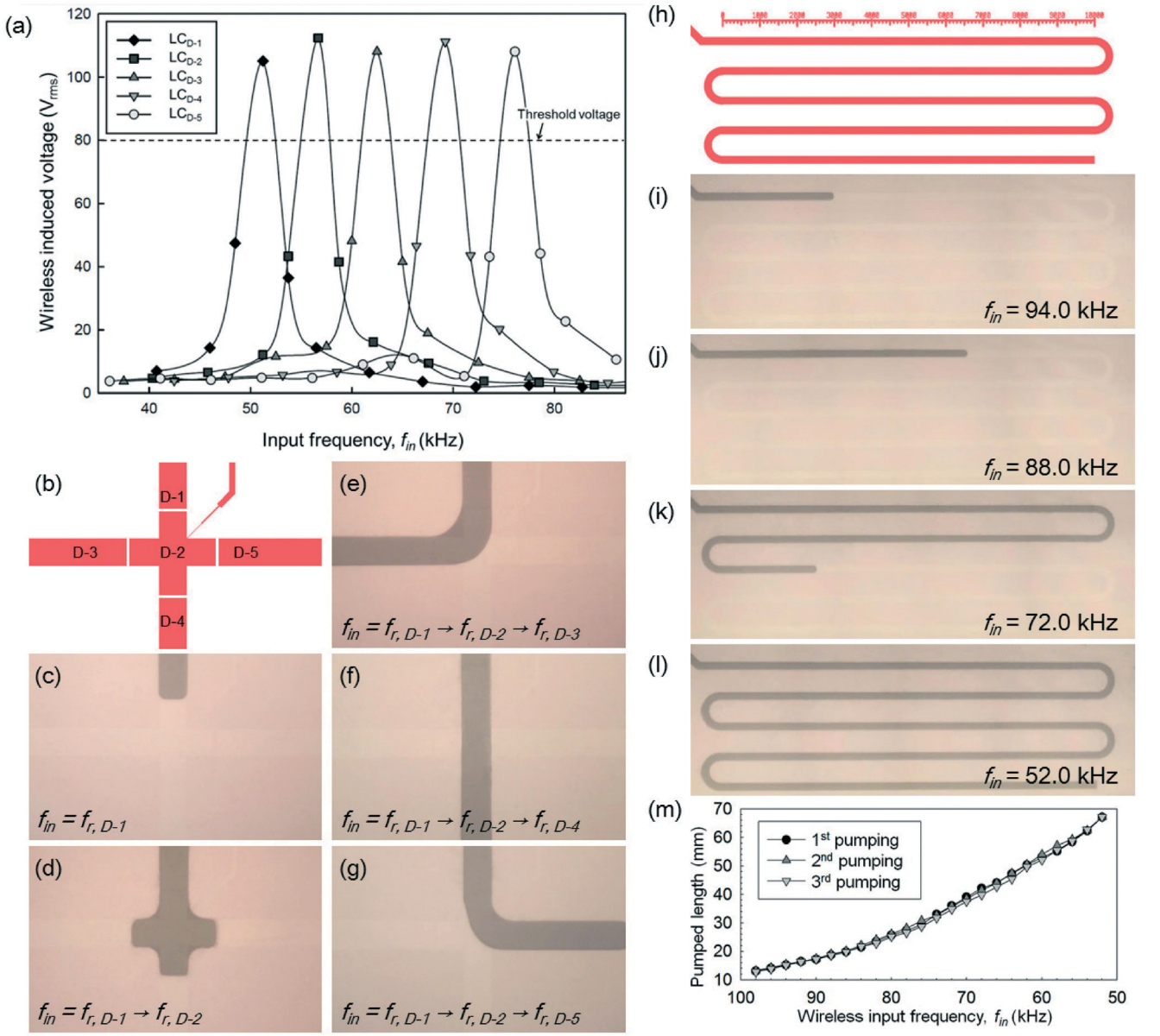

Fig. 5 Wireless DEP: (a) wireless induced voltages on 5 receiving LC circuits of the DEP device; (b) the layout design for virtual liquid channels pumping and switching; (c–g) images of pumping and switching liquid channels with different input frequencies; (h) the layout design for liquid pumping with a continuous meandered electrode; (i–l) images of liquid pumping through modulating the input frequency; (m) summarized results of the pumped liquid length at different input frequencies.

further identify the liquid pumping capability of wireless DEP. The meandered electrode with width 200 μm and length 67.1 mm is connected to a receiving LC circuit with L = 50.3 mH and C = 20.2 pF. Testing results are shown in Fig. 5(i–l). The input frequency is set as the original resonant frequency (94 kHz) initially. Then the liquid is found to be pumped for a distance about 15.2 mm and then stopped, as shown in Fig. 5(i). Since the equivalent capacitance is increased with the increasing pumped liquid between top and bottom electrodes, the resonant frequency of the receiving LC circuit becomes smaller. Then the induced voltage also becomes smaller until unable to generate the required threshold voltage for liquid pumping. To further pump the liquid forward, the input frequency is reduced to 2 kHz, then the liquid is found to be pumped forward for a distance and then stopped again. By repeating this process several times, the whole electrode length can be fully covered by the liquid, as shown in Fig. 5(j–l). The relationship between input frequency and pumping length is tested three times and summarized in Fig. 5(m). The calculated liquid capacitance based on the shift of frequency is found to be 36.8–166.0 pF, which is larger than the selected capacitance, 20.2 pF. Therefore, the resonant frequency is sensitive to the liquid capacitance. It indicates that the distance travelled by the pumped liquid using the proposed wireless DEP on a continuous electrode can be tuned by the input frequency. In other words, with a long continuous electrode design, the length of virtual liquid channel formed by DEP can be controlled through frequency modulation without using a multiple electrode design. This technique shows great potential to analogically control liquid pumping distance by DEP through frequency modulation. However, if this effect is not desired, a larger capacitance can be used for the receiving LC circuit to reduce the frequency-shift effect from variable liquid capacitance.

5. Conclusions

Here, wireless EWOD/DEP chips that are wirelessly powered and controlled through LC circuits with one-to-many transmitter–receiver coupling are designed, fabricated and tested. Each receiving LC circuit connected to the EWOD/DEP electrode is designed to have a different resonant frequency. When the input frequency is close to one of the resonant frequencies of receiving LC circuits, the induced voltage on the corresponding EWOD/DEP electrode will increase due to resonance. Therefore, electrodes can be selectively and sequentially activated to provide a sufficient EWOD or DEP force to manipulate droplet or liquid. Unlike previously reported wireless EWOD or DEP devices powered through one-to-one transmitter–receiver coupling, in our one-to-many transmitter–receiver coupling design, the transmitting inductor is much larger than the total sizes of 5 receiving inductors, therefore, receiving inductors can be easily covered and coupled by the transmitting inductor. The droplet transport, splitting, and merging are successfully demonstrated with 5 receiving LC circuits at different input frequencies (1210–1920 Hz). The liquid pumping with multiple electrodes by wireless DEP is also demonstrated with 5 receiving LC circuits at higher input frequencies (51.2–76.1 kHz). Furthermore, the liquid pumping with a continuous electrode by wireless DEP is also investigated. It is found that the length of the virtual liquid channel formed by DEP can be tuned through input frequency without using a multiple electrode design, which shows great potential to analogically control the liquid pumping distance by DEP through frequency modulation. The proposed wireless EWOD/DEP chips do not need to be physically connected with the power supply or battery. Based on this wireless EWOD/DEP technique, potential application for *in vivo* microfluidic manipulation can be further developed, such as a wireless implantable drug delivery device. However, the miniaturization of the receiving LC circuit, the wireless powering issue, and the targeting wireless distance need to be further investigated to meet specific application requirements in the future.

Acknowledgements

Part of fabrication facilities are provided by the NCTU Nano Facility Center. Authors would also like to thank Prof. Jin-Chern Chiou, Prof. Tsung-Lin Chen, Prof. and Ching-Chung Yin for providing the measurement facilities.

References

1 C. M. Ho, C. J. Kim and J. Gong, *Micro/Nano Technology Systems for Biomedical Applications, Microfluidics, Optics, and Surface Chemistry*, Oxford University Press, Oxford, UK, 2010.
2 S.-Y. Teh, R. Lin, L.-H. Hung and A. P. Lee, *Lab Chip*, 2008, **8**, 198–220.
3 S. K. Cho, H. Moon and C.-J. Kim, *J. Microelectromech. Syst.*, 2002, **12**, 70–80.
4 W. C. Nelson and C.-J. Kim, *J. Adhes. Sci. Technol.*, 2012, **26**, 1747–1771.
5 S. K. Chung, K. Rhee and S. K. Cho, *Int. J. Precis. Eng. Manuf.*, 2010, **11**, 6.
6 H. A. Pohl, *Dielectrophoresis*, Cambridge University Press, New York, 1978.
7 L. Zheng, J. P. Brody and P. J. Burke, *Biosens. Bioelectron.*, 2004, **20**, 606–619.
8 K. D. Hermanson, S. O. Lumsdon, J. P. Williams, E. W. Kaler and O. D. Velev, *Science*, 2001, **294**, 1082–1086.
9 P. Y. Chiou, A. T. Ohta and M. C. Wu, *Nature*, 2005, **436**, 370–372.
10 S.-K. Fan, W.-J. Chen, T.-H. Lin, T.-T. Wang and Y.-C. Lin, *Lab Chip*, 2009, **9**, 1590–1595.
11 Y. Mita, Y. Li, M. Kubota, W. Parkes, L. I. Haworth, B. W. Flynn, J. G. Terry, T.-B. Tang, A. D. Ruthven, S. Smith and A. J. Walton, *The 38th European Solid-state Device Research Conference*, 2008, pp. 306–309.
12 Y. Mita, Y. Li, M. Kubota, S. Morishita, W. Parkes, L. I. Haworth, B. W. Flynn, J. G. Terry, T.-B. Tang, A. D. Ruthven, S. Smith and A. J. Walton, *Solid-State Electron.*, 2009, **53**, 798–802.

13 K. Ryu, J. Zueger, S. K. Chung and S. K. Cho, *The 23rd IEEE International Conference on Micro Electro Mechanical Systems*, 2010, pp. 160–163.
14 S. H. Byun, M.-G. Yoon and S. K. Cho, *The 16th International Conference on Miniaturized Systems for Chemistry and Life Sciences*, 2012, pp. 344–346.
15 S. H. Byun and S. K. Cho, *Heat Transfer Eng.*, 2013, **34**, 140–150.
16 M. G. Yoon, S. H. Byun and S. K. Cho, *Lab Chip*, 2013, **13**, 662–668.
17 W. Qiao, G. Cho and Y.-H. Lo, *Lab Chip*, 2011, **11**, 1074–1080.
18 B. Berge, *Comptes Rendus de l'Academie des Sciences Serie II*, 1993, **317**, 157–163.
19 T. B. Jones, M. P. Perry and J. R. Melcher, *Science*, 1971, **174**, 1232–1233.
20 T. B. Jones and J. R. Melcher, *Phys. Fluids*, 1973, **16**, 393–400.
21 T. B. Jones, J. D. Fowler, Y. S. Chang and C.-J. Kim, *Langmuir*, 2003, **19**, 7646–7651.
22 T. B. Jones, K.-L. Wang and D.-J. Yao, *Langmuir*, 2004, **20**, 2813–2818.
23 K.-L. Wang and T. B. Jones, *J. Micromech. Microeng.*, 2004, **14**, 761–768.
24 T. B. Jones, M. Gunji, M. Washizu and M. J. Feldman, *J. Appl. Phys.*, 2001, **89**, 1441–1448.
25 R. Ahmed and T. B. Jones, *J. Micromech. Microeng.*, 2007, **17**, 1052–1058.
26 S.-K. Fan, T.-H. Hsieh and D.-Y. Lin, *Lab Chip*, 2009, **9**, 1236–1242.
27 S.-K. Fan, P.-W. Huang, T.-T. Wang and Y.-H. Peng, *Lab Chip*, 2008, **8**, 1325–1331.
28 Texas Instruments (Dallas, Texas, USA), operational amplifier OPA454 datasheet, http://www.ti.com/lit/ds/symlink/opa454.pdf.